8th International Symposium on Magnetic Bearing
August 26-28, 2002, Mito, Japan

DESIGN AND ROTOR DYNAMIC MODELING OF HIGH SPEED MILLING SPINDLE SUPPORTED WITH AMB

Hyeong-Joon Ahn
Dept. of Mechanical and Aerospace Eng., University of Virginia, Charlottesville, VA, 22904, USA,
hja4n@virginia.edu

In-Hwang Park, Jong-Hyuk Kim and Dong-Chul Han
School of Mechanical and Aerospace Eng., Seoul National University, Seoul, 151-742, Korea,
zeus@amed.snu.ac.kr, slim@amed.snu.ac.kr and dchan@amed.snu.ac.kr

ABSTRACT

This paper discusses design and detail modeling procedure of an accurate rotor dynamic model of high speed milling spindle supported with AMB. A fine tuning of rotor dynamic model for the AMB rotor is needed since the AMB rotor has many interference fitted parts such as laminated rotors and high speed AC motor. In addition, the draw bar equipped with springs and gripper assembled in the inner diameter of spindle with high pre load. Furthermore, the tool and tool holder can be changed considerably according to specific applications. Therefore, it is very difficult to acquire the accurate numerical mode. To get accurate mathematical model with FEM, three types of model are introduced. The first model is the spindle without draw bar, the second the spindle with draw bar and the last model the spindle with tool holder. The obtained accurate rotor dynamic model can be used as a good nominal model for the high performance controller and it can contribute to the precise estimation of the parameter variation due to tool and tool holder change without experiments.

INTRODUCTION

High speed machining (HSM) is now recognized as one of the key manufacturing technologies for higher productivity and throughput. And HSM is characterized by advantages such as decreased cutting force, high chip removal rate, low temperature increase, minimum reaction forces, and excellent surface quality. HSM creates special demands on the machine tool design, the components and the numerical control. One of key technologies for HSM is the high speed spindle, which means the necessity of high speed and stiff bearings. Since active magnetic bearing (AMB) has several advantages such as high rotational speed, active vibration control, high efficiency and long life due to no wear, and high reliability with process monitoring and diagnostics, AMB is perfectly suitable for HSC operations [1, 2].

AMB machine tools spindle consisted of interference fitted spindle, draw bar with spring, tool holder and tool. Fine tuning of rotor dynamic model for the AMB rotor is needed since the AMB rotor has many interference fitted parts such as laminated rotors and high speed AC motor. Also the draw bar equipped with springs and gripper assembled in the inner diameter of spindle with high pre load. Furthermore, the tool and tool holder can be changed considerably according to specific applications. Therefore, it is very difficult to acquire the accurate numerical model [3, 4].

Authors designed and manufactured a high speed machine tools spindle supported with AMBs [5]. The spindle has several unique features dislike existing AMB machine tools spindle:

1. Three radial sensors and two radial bearings : more rigid than three bearing design [2], high modal observability than two sensor design[6], the measurement of radial error motion closest to tools.
2. Cylindrical capacitive sensor : high precision and robustness to geometric errors [7]
3. Draw bar with coil spring: less unbalance in high speed rotation.
4. Differential measurement of entire area of thrust disk : insensitivity to geometric error.

To get accurate mathematical model with FEM [8], three types of model are introduced. The first model is the spindle without draw bar, the second the spindle with draw bar and the last model the spindle with tool holder. The second model is based

on the first model and the last model is based on the second. In the first model, we tune finely the effective bending diameter at the location of the interference fit. In the second model, we adjust the draw bar model and connecting stiffness. The coil spring contributed to increase of effective bending diameter of draw bar due to the high preload. In the third model, we model the tool holder and validate the overall model. At each stage, the impulse tests are performed to match the numerical model with real spindle. Since the mode shapes of each model are changed according to the change of mass distribution, the mode shapes of first and second model are almost same. However, the mode shape of third model with tool holder differs from other models. Although the frequency responses from impulse data are considerably different, the normalized mode shapes are not significantly different. It is noticed that the natural frequency is more important than the mode shape, even if the mode shape contributes the input and output matrices of state-space model. The obtained accurate rotor dynamic model can be used as a good nominal model for the high performance controller and it can contribute to the precise estimation of the parameter variation due to tool and tool holder change without experiments.

AMB MILLING SPINDLE DESIGN

AMB and Sensor Configuration

There were two configurations in AMB spindle, which are two bearings and three bearings shown in Figure 1 (a) and (b), respectively. The configuration of two bearings is simple and gives rigid rotor design, but this configuration can have weak observability or controllability of bending modes. And the configuration of three bearings has good controllability and observability of bending modes, but this configuration is intrinsically complex and gives flexible rotor.

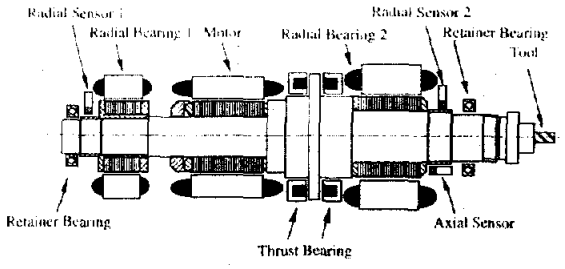

(a) Two bearings design [6]

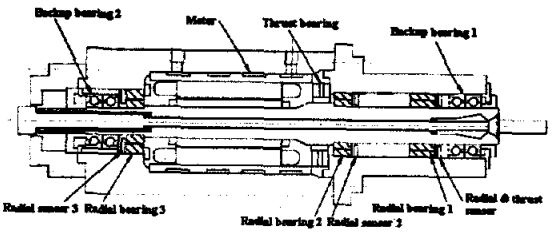

(b) Three bearings design [2]

FIGURE 1: The conventional configuration of AMB spindle

So, author propose a new configuration, three sensors and two bearings. Proposed configuration is shown in Figure 2.

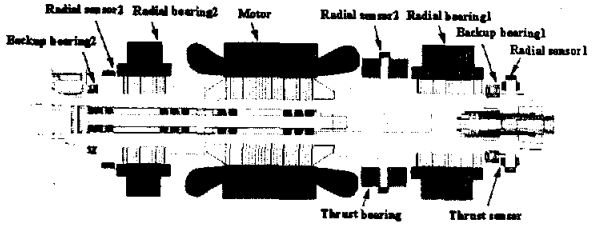

FIGURE 2: New configuration of three sensors and two bearings

This configuration gives several advantages as follows.

1. More rigid rotor and higher natural frequency than three bearing design
2. Higher modal observability than the configuration of two bearings
3. Radial and axial vibration measurement very close to tools is available.
4. Comparison of control performance between conventional and new design through the interpolation of first two sensors

Tooling

The general formula below calculates the approximate maximum *rpm* for HSK (Hohl Shank Kegel, hollow shaft taper)-clamping units in high-speed spindles. HSK 50E for high speed (Max. 40,000 *rpm*) is selected as a tool clamping system. The clamping force is 11 *kN* and spring force is 3.3 *kN*. We adopt two ultra high stiffness coil spring and the moving part between coil springs gives more accurate concentricity. Draw bar has through hole for compressed air to clean the HSK taper and front side of spindle. Figure 3 shows the HSK hydraulic milling chuck and draw bar equipped with coil spring and HSK gripper are shown. The load reducer for avoiding excessive load

to front backup bearing in clamping the tool is introduced. For ATC (Automatic tool change), pneumatic actuator consisting of three pistons and cylinders is equipped with the proximity sensors. The pneumatic cylinder for ATC is shown in Figure 4.

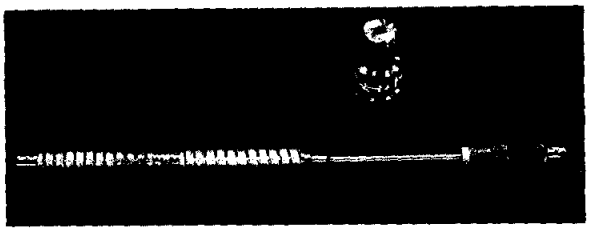

FIGURE 3: Draw bar and HSK tool holder

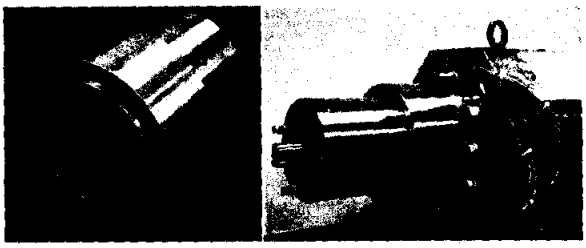

(a) Pneumatic cylinder (b) Assembly

FIGURE 4: The pneumatic cylinder for ATC

Bearing design

Non-oriented silicon steel is selected as the laminated radial bearing and laminated rotor materials. Considering the safety factor, the saturation flux density is chosen as 1.5 *T*. The radial bearing is designed considering the below specifications.

Front bearing design specification F_{max} = 1500 *N*, F_{RMS} = 1000 *N*, Slew rate = 2e10^6 *N/sec*, g = 0.25 *mm*, γ = 0.7, Safety factor = 1.05, Current density = 6000,000 A/m^2, Shaft diameter = 90 *mm*

Rear bearing design specification F_{max} = 1000 *N*, F_{RMS} = 700 *N*, Slew rate = 1.5e10^6 *N/sec*, g = 0.25 *mm*, γ = 0.7, Safety factor = 1.05, Current density = 6000,000 A/m^2, Shaft diameter = 90 *mm*

Thrust bearing design specification B_{sat} = 1.60 *T*, F_{max} = 2000*N*, g = 0.5 *mm*, Current density = 10,000,000A/m^2.

For simplicity and mechanical strength, 8 legs configuration is selected. The photos of assembled radial bearings are shown in Figure 5(a). The pole of thrust bearing and the thrust disk of the spindle are designed in order that maximum deflection to axial direction is less than 1 μm at maximum load condition using commercial FEM software. Resulting thrust bearing is shown in Figure 5(b).

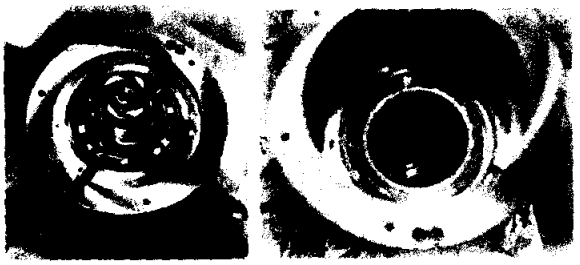

(a) Front bearing (b) Rear bearing

FIGURE 5: Assembled front and rear bearings

Sensor design

Three radial CCS and differential thrust capacitive sensor are adopted in this AMB spindle. Front and rear CCS are exactly same shapes and the middle CCS is design to have same displacement gain as the front CCS. Front CCS and thrust capacitive sensor is located as near tool as possible to reduce the effect of thermal expansion and to measure the spindle vibration near tool. The front radial and thrust sensors are shown in Figure 6. To make spindle rigid, the middle radial sensor is equipped in thrust bearing housing and rear radial sensor is equipped in rear bearing. The middle and rear radial sensors are shown in Figure 7.

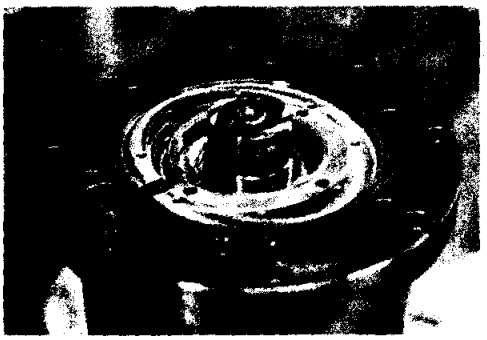

FIGURE 6: Front radial and thrust sensors

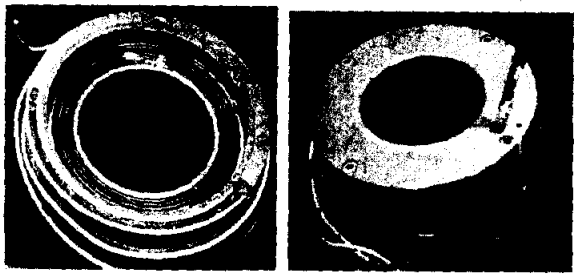

(a) Middle radial sensor (b) Rear radial sensor

FIGURE 7: Middle and rear radial sensors

OVERALL SYSTEM DESCRIPTION

The schematics of designed AMB spndle and main component descriptions are shownin Figure 8. The primary distictions of this AMB spindle are the new configration of three sensors and two bearings, the load reducer of avoiding the excessive tooling load of back up and thrust bearings, the axial cooling jacket instead of spiral one for the efficient usage ofhousing as well as for the cooling of AMB and the adoption of coil spring for clamping force, as shown in Figure 8.

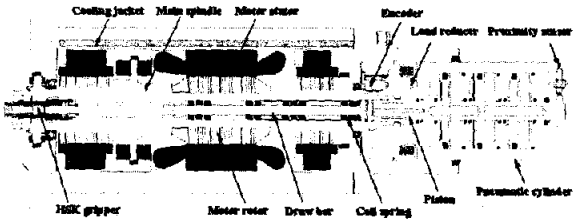

FIGURE 8: Schematics of AMB spindle

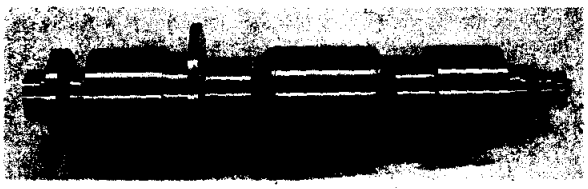

FIGURE 9: Spindle

The photos of spindle is shown in Figure 9. All rotors except of thrust sensor disk and load reducer are fringe-fitted.

The assembled housing are shown in Figure 10 (a). The designed AMB spindle is very similar with ordinary spindle except the bearing and sensor wires. A few holes on the housing are made for sensor and bearing wiring. The Overall system equipped in horizontal main housing is shown in Figure 10 (b). The flange type spindle is assembled in horizontal main housing.

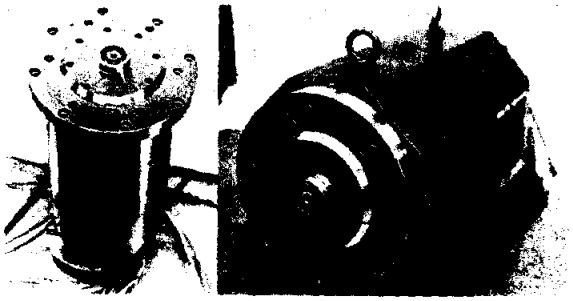

(a) Side view (b) Perspective view

FIGURE 10: The assembled housing

ROTOR DYNAMIC MODELING

To get accurate mathematical model, three types of models are introduced. The first model is the spindle without draw bar, the second the spindle with draw bar and the last model the spindle with tool holder. The second model is based on the first model and the last model is based on the second. The first FEM model of the spindle without draw bar is shown in Figure 11. This model is to determine the bending diameter of interference fitted part

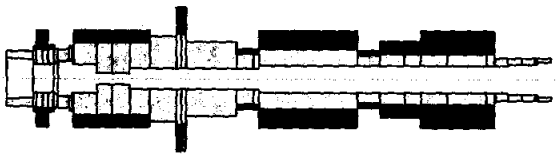

FIGURE 11: The FEM model of spindle without draw bar

The bending diameter increases by about one over five times of the difference between outer and inner diameter of interference-fitted part in this case although the bending diameter increase depends on the interference-fit clearance. The impulse tests are performed to validate the FEM model. The node points of impulse test are determined, considering the estimated mode shape of the spindle and the location of bearing and sensor. The node points for impulse test are shown in Figure 12.

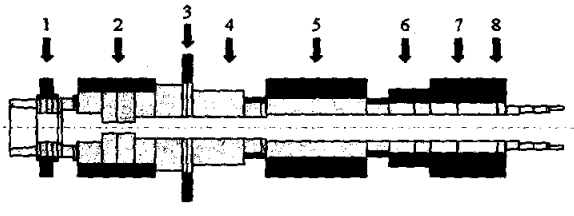

FIGURE 12: Node points for impulse test

The 1, 3 and 8 nodal points are the sensor locations, the 2 and 7 nodal points the bearing locations and the 4, 5 and 6 the nodal points are chosen considering estimated mode shape. The transfer functions are measured with HP dynamic analyzer 35670A, Kistler impulse hammer 9904A, and accelerometer 8452A. The number of modes included in these models was based on the desire to actively control the rotor up to certain bandwidth. Therefore, for evaluation of the reduced models the frequency range of interest was chosen to be from 0 to 3 *kHz*, which is slightly higher that controller bandwidth. The 8 points of impulse excitation and 8 points of measurement gives 8x8, 64 measured response.

The appropriate collection of impulse response results in six 3D plots of impulse test, which gives the insight of the mode shapes and modal characteristics. The 3D plot of impulse test response of the first model from 4th nodal point to all points is shown in Figure 13.

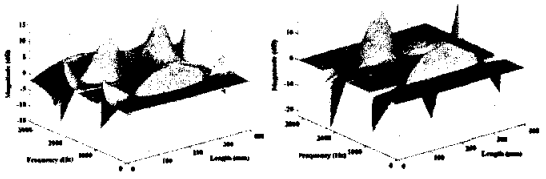

(a) Real part (b) Imaginary part

FIGURE 13: 3D mode shape of the 1st model with impulse test in node number 4

The second model is shown in Figure 14. The draw bar model is added to the first model. The draw bar and the first mode are interconnected with 10 radial links. The radial link is located on the nodes of metallic contact. The draw bar modes doesn't appear in combined model due to radial links. The bending diameter of draw bar increases due to the coil spring for clamping force. The natural frequency of the first bending mode decreases considerably while that of second bending mode doesn't decrease much due to the stiffness of draw bar. The impulse test is also performed in the same node points as the first model to tune and validate the FEM model. The 3D plot of impulse test response from 4th nodal point to all points is shown in Figure 15. The 3D plot of impulse test data of the second model is very similar with the first model.

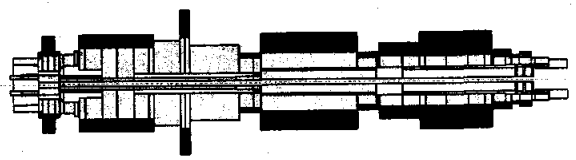

FIGURE 14: The FEM spindle model with draw bar

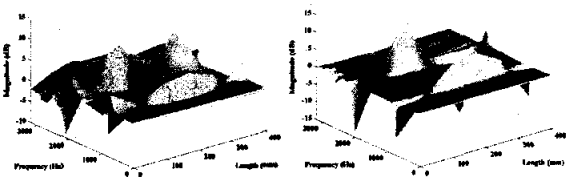

(a) Real part (b) Imaginary part

FIGURE 15: 3D mode shape of the 2nd model with impulse test in node number 4

The last FEM model is the spindle with tool holder as shown in Figure 16. Since the HSK tooling is based on the elastic deformation of tool holder, the tool holder is included in the spindle model instead of introducing another rotor. The 3D plot of impulse test response from 4th nodal point to all points is shown in Figure 17. The tool holder significantly changes the frequency response.

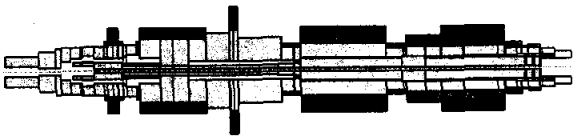

FIGURE 16: The FEM model of spindle with tool holder

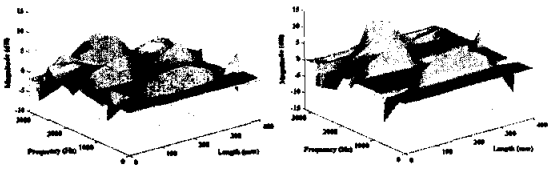

(a) Real part (b) Imaginary part

FIGURE 17: 3D mode shape of the 3rd model with impulse test in node number 4

The measured modes shapes of three models on the 4th node are shown in Figure 18. Since the mode shapes of each model are changed with the change of mass distribution, the mode shapes of first and second model are almost same. However, the mode shape of third model with tool holder differs from other models

slightly. Also, the difference in the second bending mode is bigger than that in the first bending mode. Although the frequency responses from impulse data are significantly different, the normalized mode shapes are not significantly different. It is noticed that the natural frequency is more important than the mode shape, even if the mode shape contributes the input and output matrices of state-space model.

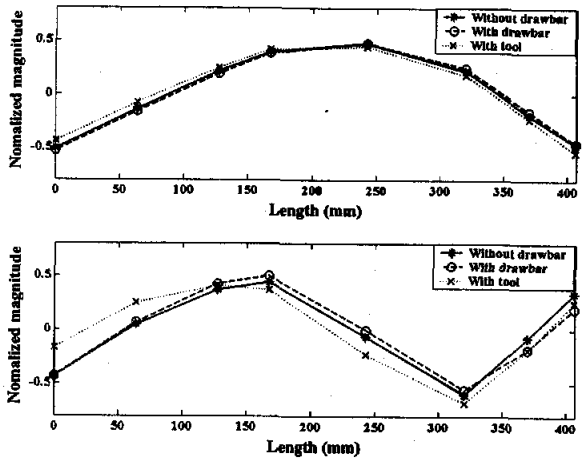

FIGURE 18: The comparison of measured and theoretical mode shapes of three models

The measured and theoretical natural frequencies are shown in Table 1. The theoretical model match with measured data very well.

TABLE 1 Theoretical and measured natural frequencies

	1^{ST} bending (Hz)		2^{ND} bending (Hz)	
	FEM	Impulse	FEM	Impulse
Spindle without draw bar	678.8	680	1763	1764
Spindle with draw bar	750.53	752	2032.7	2032
Spindle with tool holder	812.77	812	2156.8	2156

CONSLUSION

Authors designed and manufactured a high speed machine tools spindle supported with AMBs. To get accurate mathematical model with FEM, three types of model are introduced. The first model is the spindle without draw bar, the second the spindle with draw bar and the last model the spindle with tool holder. The second model is based on the first model and the last model is based on the second. In the first model, we tune finely the effective bending diameter at the location of the interference fit. In the second model, we adjust the draw bar model and connecting stiffness. The coil spring contributed to increase of effective bending diameter of draw bar due to the high preload. In the third model, we model the tool holder and validate the overall model. At each stage, the impulse tests are performed to match the numerical model with real spindle. It is noticed that the natural frequency is more important than the mode shape, even if the mode shape contributes the input and output matrices of state-space model. The obtained accurate rotor dynamic model can be used as a good nominal model for the high performance.

REFERENCE

1. Schulz , H. and Moriwaki, T., "High-Speed Machining," Annals of the CIRP, Vol. 41, Feb, 1992, PP. 637–643.
2. Stephens, L. S., "Design and Control of Active Magnetic Bearings for a High Speed Machining Spindle," Ph. D. dissertation, University of Virginia, Aug. 1995.
3. Schweitzer, G., Bleuler, H. and Traxler, A., "Active Magnetic Bearings," Hochschulverlag AG de ETH Zürich, Switzerland, 1994.
4. Antkowiak, B. M., Nelson, F. C. "Rotor dynamic modeling of an Actively Controlled Magnetic Bearing Gas Turbine Engine," J. of Engineering for Gas Turbines and Power, Vol. 120, 1998, pp. 621-625.
5. Ahn, H. J., "A Study on System Identification and Vibration Control of the AMB Spindle for High Speed Precision Machining Using Cylindrical Capacitive Sensors," Ph.D. dissertation, Seoul National University, Korea., 2001.
6. Siegwart, R., Larsonneur, R. and Traxler, A., "Design and Performance of a High Speed Milling Spindle in digitally Controlled Active Magnetic Bearings," Proceedings of the 2^{nd} ISMB, Tokyo, Japan, July, 1990, pp. 197-204.
7. Ahn, H. J., Jeon, S., & Han, D. C. "Error Analysis of the Cylindrical Capacitive Sensor for Active Magnetic Bearing Spindles," J. of Dynamics Systems, Measurement and Control, Trans. of ASME, March, Vol. 122, 2000, pp. 102-107
8. RODAP (ROtating machine Design and Analysis Program), D&M Technology Co., Korea.